

In vivo PET imaging with [¹⁸F]FDG to explain improved glucose uptake in an apolipoprotein A-I treated mouse model of diabetes

Blake J. Cochran¹ · William J. Ryder^{2,3} · Arvind Parmar⁴ · Shudi Tang¹ ·
Anthonin Reilhac^{3,4} · Andrew Arthur⁴ · Arnaud Charil^{3,4} · Hasar Hamze⁴ ·
Philip J. Barter^{1,5} · Leonard Kritharides^{5,6} · Steven R. Meikle^{2,3} ·
Marie-Claude Gregoire⁴ · Kerry-Anne Rye^{1,5}

Received: 21 February 2016 / Accepted: 27 April 2016 / Published online: 18 May 2016
© Springer-Verlag Berlin Heidelberg 2016

Abstract

Aims/hypothesis Type 2 diabetes is characterised by decreased HDL levels, as well as the level of apolipoprotein A-I (apoA-I), the main apolipoprotein of HDLs. Pharmacological elevation of HDL and apoA-I levels is associated with improved glycaemic control in patients with type 2 diabetes. This is partly due to improved glucose uptake in skeletal muscle.

Methods This study used kinetic modelling to investigate the impact of increasing plasma apoA-I levels on the metabolism of glucose in the *db/db* mouse model.

Results Treatment of *db/db* mice with apoA-I for 2 h significantly improved both glucose tolerance ($AUC\ 2574 \pm 70\ \text{mmol/l} \times \text{min}$ vs $2927 \pm 137\ \text{mmol/l} \times \text{min}$, for apoA-I and PBS, respectively; $p < 0.05$) and insulin sensitivity ($AUC\ 388.8 \pm 23.8\ \text{mmol/l} \times \text{min}$ vs $194.1 \pm 19.6\ \text{mmol/l} \times \text{min}$, for apoA-I and PBS, respectively; $p < 0.001$). ApoA-I treatment also increased glucose uptake by skeletal muscle in both an insulin-dependent and insulin-independent manner as evidenced by increased uptake of fludeoxyglucose ([¹⁸F]FDG) from plasma into gastrocnemius muscle in apoA-I treated mice, both in the

absence and presence of insulin. Kinetic modelling revealed an enhanced rate of insulin-mediated glucose phosphorylation (k_3) in apoA-I treated mice ($3.5 \pm 1.1 \times 10^{-2}\ \text{min}^{-1}$ vs $2.3 \pm 0.7 \times 10^{-2}\ \text{min}^{-1}$, for apoA-I and PBS, respectively; $p < 0.05$) and an increased influx constant ($3.7 \pm 0.6 \times 10^{-3}\ \text{ml}\ \text{min}^{-1}\ \text{g}^{-1}$ vs $2.0 \pm 0.3 \times 10^{-3}\ \text{ml}\ \text{min}^{-1}\ \text{g}^{-1}$, for apoA-I and PBS, respectively; $p < 0.05$). Treatment of L6 rat skeletal muscle cells with apoA-I for 2 h indicated that increased hexokinase activity mediated the increased rate of glucose phosphorylation.

Conclusions/interpretation These findings indicate that apoA-I improves glucose disposal in *db/db* mice by improving insulin sensitivity and enhancing glucose phosphorylation.

Keywords Diabetes · FDG · Glucose uptake · Insulin sensitivity · Kinetic modelling

Abbreviations

apoA-I	Apolipoprotein A-I
CT	Computed tomography
FDG	Fludeoxyglucose
HK-II	Hexokinase II
PET	Positron emission tomography
PI3K	Phosphatidylinositol-3 kinase
PKA	Protein kinase A
PSF	Point spread function
ROI	Region of interest
SR-BI	Scavenger receptor class B type I

Introduction

Type 2 diabetes is characterised by decreased HDL-cholesterol levels, as well as a decreased level of apolipoprotein A-I (apoA-I), the main HDL apolipoprotein [1].

✉ Blake J. Cochran
b.cochran@unsw.edu.au

¹ School of Medical Sciences, Faculty of Medicine, UNSW Australia, Sydney 2052, NSW, Australia

² Faculty of Health Sciences, University of Sydney, Sydney, NSW, Australia

³ Brain and Mind Centre, University of Sydney, Sydney, NSW, Australia

⁴ ANSTO LifeSciences, Sydney, NSW, Australia

⁵ Faculty of Medicine, University of Sydney, Sydney, NSW, Australia

⁶ Department of Cardiology, Concord Repatriation General Hospital, Sydney, NSW, Australia

Therapeutic interventions that increase plasma HDL levels improve glycaemic control in patients with type 2 diabetes [2, 3], and treatment with HDL or apoA-I has been shown to increase glucose uptake into skeletal muscle [4, 5] and adipose tissue [6]. Furthermore, treatment with HDL or apoA-I increases insulin secretion and production in isolated pancreatic islets and insulinoma beta cell lines [7, 8]. Recent studies have demonstrated that both single and repeated doses of apoA-I can also improve insulin resistance in fat-fed C57Bl6 mice [9, 10], as can overexpression of apoA-I [11].

Here, we have established a methodology using [^{18}F]FDG and positron emission tomography/computed tomography (PET/CT) imaging, together with kinetic modelling, to quantify the in vivo, real-time impact of apoA-I treatment on glucose uptake into skeletal muscle. The *db/db* mouse is a well-established animal model of type 2 diabetes [12]. While previous studies have been conducted using [^{18}F]FDG to examine glucose uptake in *db/db* mice as an insulin resistant animal model, these studies only quantified endpoint uptake in the heart [13] and cardiac and skeletal muscle [14] and did not extend to determination of kinetics. Kinetic modelling of PET dynamic studies permits analysis beyond simple characterisation of global glucose uptake and determines the glucose influx and phosphorylation rates in specific tissues.

Methods

Mice B6/BKS(D)-*Lepr^{db}/J* (*db/db*) mice were obtained from The Jackson Laboratory (Bar Harbor, ME, USA). The experiments were conducted on 6-week-old male homozygous mice maintained on standard chow in pathogen-free conditions. All procedures were approved by the Sydney Local Health District and University of Sydney Animal Ethics Committees and followed the NIH *Guide for the care and use of laboratory animals*, Eighth edition (2011). Mice were randomly assigned to treatment groups by coin flip.

ApoA-I treatment Mice received a single i.p. injection of human apoA-I (40 mg/kg, CSL Pty, Parkville, Australia) or an equivalent volume of PBS ($n=5$ /group). Blood was sampled from the lateral tail vein over 24 h and plasma apoA-I concentrations were determined by an ELISA that was specific for human apoA-I (Cell Biolabs, San Diego, CA, USA).

Glucose tolerance test Mice were fasted for 3 h prior to receiving human apoA-I (40 mg/kg i.p.) or an equivalent volume PBS ($n=7$ /group). After a further 2 h, glucose (1 g D-glucose/kg; Sigma-Aldrich, St Louis, MO, USA) was injected i.p. Blood glucose levels were determined using an Accu-Chek Performa glucometer (Roche, Basel, Switzerland).

Insulin tolerance test Random fed mice received a single i.p. injection of human apoA-I (40 mg/kg) or PBS ($n=6$ /group). After a further 2 h insulin (3 U human insulin/kg; Sigma-Aldrich) was injected i.p. and blood glucose levels measured as above.

Ex vivo skeletal muscle glucose uptake Fasted mice were treated with apoA-I (40 mg/kg i.p.) or PBS ($n=6$ /group) and euthanised 2 h later. The gastrocnemius muscle was removed and 2-deoxy[^3H]glucose (PerkinElmer, Waltham, MA, USA) uptake was quantified [15]. The muscle was incubated for 1 h at 37°C with or without insulin (0.3 $\mu\text{mol/l}$), transferred to fresh buffer containing 1 mmol/l 2-deoxy[^3H]glucose (37 kBq/ml) and 7 mmol/l D-[^{14}C]mannitol (14.8 kBq/ml; PerkinElmer) with or without insulin (0.3 $\mu\text{mol/l}$) for 10 min. Glucose uptake was terminated by immersion in ice-cold buffer containing 80 $\mu\text{mol/l}$ cytochalasin B (Sigma-Aldrich). White and red muscle was isolated, snap frozen in liquid nitrogen and stored at -80°C for further use. Muscle samples were homogenised, and the ^3H and ^{14}C content determined by liquid scintillation counting.

Small-animal PET study Fasted mice received an i.p. injection of apoA-I (40 mg/kg) or PBS ($n=4$ /group). After 2 h, the mice were anaesthetised with isoflurane administered via precision vaporiser (induction, 5%; maintenance, 1.5–2%), and maintained in a surgical plane of anaesthesia for the duration of the procedure. For mice treated with insulin, a dose of 3 U human insulin/kg was administered s.c. 30 min before the start of the PET/CT scan. After positioning the mice in the gantry of an Inveon PET/CT Scanner (Siemens, Munich, Germany), a 60 min PET scan commenced immediately after injection of [^{18}F]FDG (10–18 MBq, pH 6.6–7.0, 0.1 ml; PETNET Solutions, Lucas Heights, Australia) via the lateral tail vein. After completing the PET scan, a CT scan was performed to allow the co-registration of radiotracer uptake with tissues.

Image reconstruction Image reconstruction was performed using IAW 2.02 (Siemens). The listmode data was histogrammed into 16 frames (6 \times 10 s, 4 \times 60 s, 1 \times 300 s, 5 \times 600 s) for the period 0–60 min after tracer injection. Emission sinograms were reconstructed using 2D-filter back projection with a zoom of 1.5. The reconstructed images consisted of 16 frames of a 128 \times 128 \times 159 matrix with a voxel size of 0.52 \times 0.52 \times 0.796 mm³. They were corrected for attenuation (CT-based), scatter, randoms, normalisation, isotope decay, branching ratio, deadtime and were calibrated to Bq/ml.

[^{18}F]FDG region of interest Regions of interest (ROIs) (gastrocnemius muscle and inferior vena cava) were drawn on the image volumes using Brain-Visa/Anatomist version 3.1 (<http://brainvisa.info/web/index.html>) and time-activity

curves were extracted from the dynamic frames. Radioactivity uptake values were quantified in Bq per cubic cm of tissue, and converted into the percentage of injected dose per cubic cm.

Input function The input function was derived from the image by placing an ROI over the inferior vena cava. Due to the size of the vena cava in a mouse, it is necessary to correct for the system point spread function (PSF). This was achieved by using the reblurred Van Cittert deconvolution method [16] and deconvolving the estimated system PSF for five iterations. Post deconvolution images were used to create an input function time–activity curve from dynamic frames. The FDG two-tissue compartment model requires the plasma input function. The blood input function was converted to the plasma input function using the following equation [17]:

$$\text{Input_plasma} = \text{Input_blood} \times (0.386e^{-0.191t} + 1.165)$$

Modelling The FDG two-tissue compartment method with $k_4=0$ was used for modelling. The blood, plasma and gastrocnemius total activity counts were loaded into PMOD, version 3.17 (PMOD Technologies, Zürich, Switzerland) and the FDG model fitted. During fitting of the parameters, the V_b (blood volume fraction) was initially fixed at 2%, and dispersion effect [18] was applied to the input functions as proposed by Oikonen [19]. The optimum value for dispersion was found by minimising the χ^2 value for the FDG model. A final fit was made using a floating V_b and the optimised dispersion value, this yielded the rate constants (k_1 – k_3) and influx constant was calculated as $K_1=(k_1 \times k_3)/(k_2+k_3)$. The researcher conducting the kinetic modelling was blinded to treatment groups.

Cell culture L6 rat skeletal muscle cells were cultured at 37°C in a humidified, 5% CO₂ atmosphere with α -MEM medium supplemented with 10% (vol./vol.) FCS. Cells were differentiated as previously described [6].

Hexokinase activity assay Cells were serum starved for 6 h prior to treatment with apoA-I (final concentration 1 mg/ml) or equivalent volume PBS. After 1.5 h, cells were treated with insulin (final concentration 0.1 μ mol/l) or equivalent volume PBS for a further 30 min. Hexokinase activity was determined by measuring NADH production in lysates after 30 min incubation period with a hexokinase assay kit (Abcam, Cambridge, MA, USA).

GLUT4 translocation GLUT4 translocation was measured as described previously [20]. L6 cells were incubated at 37°C for 2 h with or without apoA-I (1 mg/ml). Primary anti-GLUT4, specific for the extracellular domain (1:100,

Santa Cruz Biotechnology, Dallas, TX, USA), and secondary DyLight488 donkey anti-goat (1:500, Abcam) antibodies were incubated together for 10 min at room temperature. Cells were washed with PBS and incubated with the antibody complex in the presence and absence of insulin (0.1 μ mol/l) for 30 min. Cells were analysed using a FACSverse flow cytometer (BD Biosciences, San Jose, CA, USA).

Statistical analysis All data presented are mean \pm SD. Data was analysed using Prism 6 (GraphPad, La Jolla, CA, USA). A p value <0.05 was considered statistically significant. Glucose and insulin tolerance tests were compared using unpaired, two-tailed t tests. Mann–Whitney tests were used to compare the kinetic parameters between groups. Hexokinase activity and GLUT4 translocation experiments were compared by ANOVA and a Tukey's multiple comparison test.

Results

ApoA-I increases glucose tolerance and improves insulin sensitivity in *db/db* mice At 2 h after receiving a single bolus of apoA-I (40 mg/kg i.p.) the plasma level of human apoA-I in *db/db* mice was maximal (65.24 \pm 14.42 μ g/ml), and remained relatively constant for a further 5 h (Fig. 1a). At 24 h after the injection, the apoA-I concentration had decreased to 34.85 \pm 9.68 μ g/ml. As plasma levels of apoA-I were maximal at 2 h, this time point was used in all subsequent experiments.

Treatment with apoA-I improved glucose tolerance in the *db/db* mice (white circles) compared with saline (154 mmol/l NaCl)-treated animals (black squares) (AUC 2574 \pm 70 mmol/l \times min vs 2927 \pm 137 mmol/l \times min for apoA-I and PBS treatment, respectively; $p < 0.05$) (Fig. 1b). When subjected to an insulin tolerance test, blood glucose levels (black squares) decreased by 25%, from 10.83 \pm 1.98 mmol/l to 8.13 \pm 1.97 mmol/l in the PBS-treated mice and by 43%, from 9.62 \pm 0.64 mmol/l to 5.52 \pm 1.09 mmol/l, in the apoA-I-treated mice (white circles) (AUC 388.8 \pm 23.8 mmol/l \times min vs 194.1 \pm 19.6 mmol/l \times min for apoA-I and PBS treatment, respectively; $p < 0.001$) (Fig. 1c).

ApoA-I increases ex vivo glucose uptake by skeletal muscle in *db/db* mice The ability of apoA-I to increase glucose uptake by skeletal muscle in insulin resistant *db/db* mice was also investigated. Ex vivo glucose uptake by red and white gastrocnemius muscle from PBS-treated *db/db* mice was not significantly increased by incubation with insulin (Fig. 2, black bars). When a single i.p. injection of apoA-I was administered to the animals 2 h prior to euthanasia, insulin-independent glucose uptake in red gastrocnemius muscle increased from 2.91 \pm 1.09 nmol mg⁻¹ h⁻¹ for the PBS-treated animals to 5.10 \pm 0.42 nmol mg⁻¹ h⁻¹ (Fig. 2, white bars, $p < 0.001$), while insulin-independent glucose uptake into

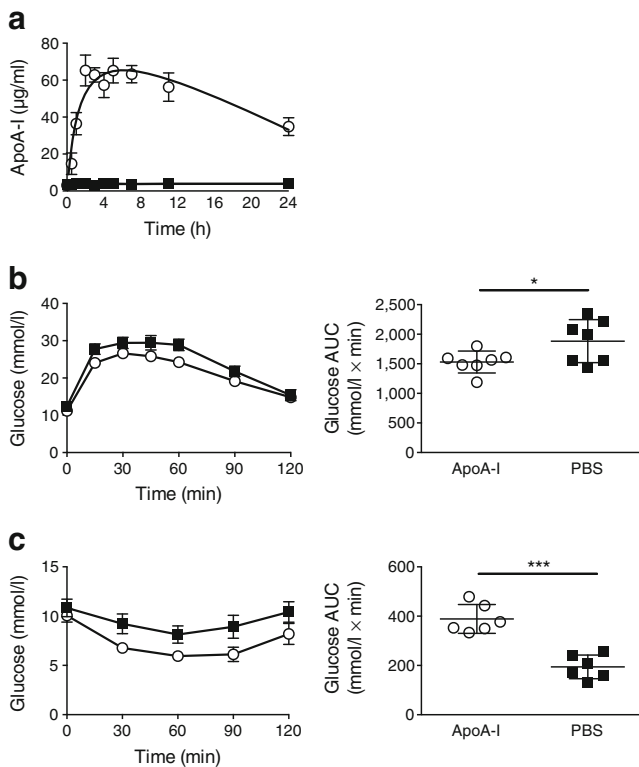


Fig. 1 ApoA-I improves glucose tolerance and insulin resistance in *db/db* mice. **(a)** Six-week-old male *db/db* mice received an i.p. injection of lipid-free apoA-I (40 mg/kg; white circles) or an equivalent volume PBS (black squares) ($n=6$ /group). Blood samples were collected from the lateral tail vein and plasma levels of human apoA-I quantified by ELISA. **(b)** Glucose tolerance test. Mice were fasted for 3 h prior to receiving an injection of apoA-I (40 mg/kg i.p.; white circles) or PBS (black squares) and after a further 2 h, 1 g/kg glucose i.p. Blood glucose levels were measured using a glucometer ($n=7$ /group). **(c)** Insulin tolerance test. Random fed mice received an injection of apoA-I (40 mg/kg i.p.; white circles) or PBS (black squares) and after 2 h, 3 U of human insulin/kg i.p. Blood glucose levels were measured as above for lipid-free apoA-I ($n=6$ /group). All values are mean \pm SD. * $p<0.05$, *** $p<0.001$

white muscle increased from 3.58 ± 1.17 nmol $\text{mg}^{-1} \text{h}^{-1}$ to 5.93 ± 1.34 nmol $\text{mg}^{-1} \text{h}^{-1}$ ($p<0.01$).

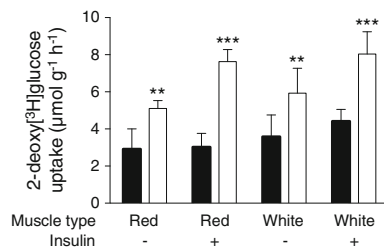


Fig. 2 ApoA-I increases glucose disposal in skeletal muscle in *db/db* mice. Male *db/db* mice were fasted for 3 h prior to receiving an i.p. injection of lipid-free apoA-I (40 mg/kg; white bars) or PBS (black bars). The mice were fasted for a further 2 h then euthanised. The gastrocnemius muscle was removed, red and white components were isolated, and glucose uptake was determined as described in the Methods section. ** $p<0.01$, *** $p<0.001$ for muscles from animals treated with apoA-I compared with muscles from animals treated with PBS

In the presence of insulin, glucose uptake into red muscle from the control animals was 3.02 ± 0.74 nmol $\text{mg}^{-1} \text{h}^{-1}$, compared with 7.63 ± 0.65 nmol $\text{mg}^{-1} \text{h}^{-1}$ in the apoA-I-treated animals ($p<0.001$). Treatment with apoA-I also increased insulin-dependent glucose uptake into white muscle from 4.41 ± 0.65 nmol $\text{mg}^{-1} \text{h}^{-1}$ in the PBS-treated animals to 8.04 ± 1.12 nmol $\text{mg}^{-1} \text{h}^{-1}$ ($p<0.01$). This indicates that treatment with apoA-I markedly improved insulin-dependent and insulin-independent glucose uptake by skeletal muscle in insulin resistant *db/db* mice.

In vivo [¹⁸F]FDG imaging of apoA-I-mediated increased glucose uptake

We next asked if the apoA-I-mediated increase in ex vivo glucose uptake could be confirmed in vivo. Mice received an intravenous infusion of [¹⁸F]FDG 2 h after apoA-I treatment. Uptake of the tracer into the gastrocnemius muscle was measured over 60 min and expressed as mean tissue [¹⁸F]FDG normalised for the dose. Early uptake of [¹⁸F]FDG into the gastrocnemius muscle was significantly increased in mice that had been pretreated with apoA-I compared with control (maximal activity at 270 s post injection; 0.93 ± 0.08 vs $1.56 \pm 0.19\%$ injected dose for PBS and apoA-I treated animals, respectively; $p<0.05$) (Fig. 3a, b). While treatment of mice with insulin 30 min before infusion of [¹⁸F]FDG altered the pattern of tracer uptake, the uptake remained higher in animals treated with apoA-I compared with PBS-treated controls (maximal activity at 450 s post injection; 1.02 ± 0.04 vs $1.35 \pm 0.05\%$ injected dose for PBS and apoA-I-treated animals, respectively; $p<0.05$) (Fig. 3c, d). While treatment with apoA-I alone had no significant impact on plasma levels of [¹⁸F]FDG relative to control (Fig. 3e), treatment of mice with apoA-I and insulin significantly increased the rate of exit of [¹⁸F]FDG from the plasma compared with mice that received only insulin (maximal activity at 55 s post injection 64.89 ± 4.45 vs $45.00 \pm 4.21\%$ of the injected dose for PBS and apoA-I-treated animals, respectively, $p<0.05$) (Fig. 3f). This increased rate of [¹⁸F]FDG clearance from the plasma likely accounts for the lower maximal uptake in animals receiving apoA-I and insulin vs apoA-I alone.

Kinetic modelling To further understand the impact of apoA-I treatment on the altered [¹⁸F]FDG uptake patterns observed in skeletal muscle and the effects on the level of the tracer in plasma, data were fitted to a two-tissue compartment, three-rate constant model (Fig. 4a), with compartments corresponding to arterial plasma [¹⁸F]FDG concentration (C_1), intracellular [¹⁸F]FDG concentration (C_2) and [¹⁸F]FDG glucose-6-phosphate intracellular concentration (C_3). Treatment with apoA-I, either in the presence or absence of insulin, did not significantly alter the rate of [¹⁸F]FDG transport from the arterial plasma to the intracellular space (k_1) (Fig. 4b), although there was a trend towards higher values in animals

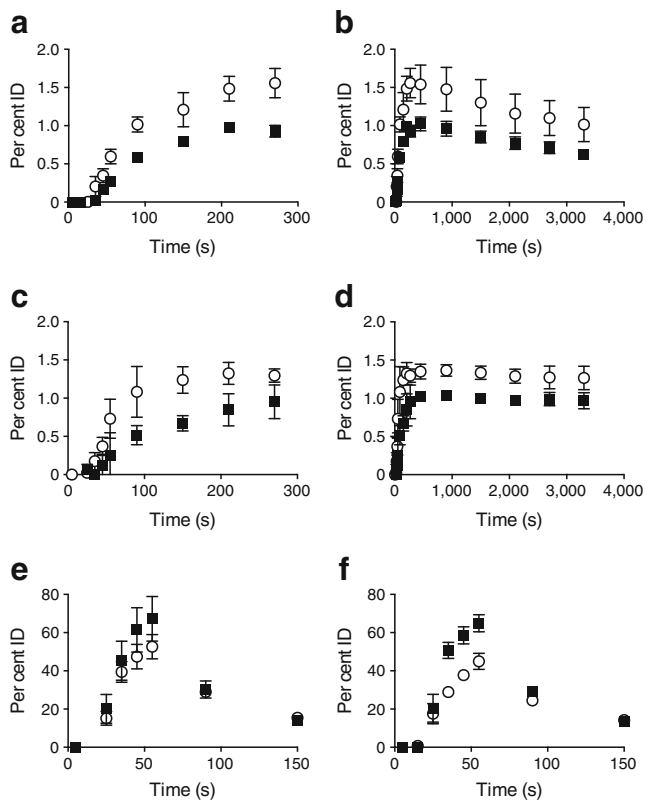


Fig. 3 Time-activity curves for ROIs in gastrocnemius muscle (a–d) and vena cava (e, f). Male *db/db* mice were fasted for 3 h prior to receiving i.p. injections of lipid-free apoA-I (40 mg/kg; white circles) or PBS (black squares). Mice were fasted for a further 2 h and then anaesthetised. Mice treated with insulin received a dose of 3 U/kg. [^{18}F]FDG (10–18 MBq) was delivered via i.v. injection and levels in the gastrocnemius muscle and vena cava determined by PET/CT for 60 min. (a) and (c) show the first 270 s of (b) and (d), respectively. Values are mean \pm SD and expressed as percentage of injected dose (ID), calculated from a full field of view ($n=4$ /group)

treated with apoA-I relative to control. Additionally, no significant change in the rate of transport from the intracellular space to plasma (k_2) was observed between treatment groups (Fig. 4c). Insulin treatment alone significantly increased the rate of [^{18}F]FDG phosphorylation (k_3) ($7.06 \pm 6.60 \times 10^{-3}$ vs $2.260 \pm 0.72 \times 10^{-2} \text{ min}^{-1}$ for PBS and PBS insulin-treated groups, respectively; $p < 0.05$) (Fig. 4d). While treatment with apoA-I alone had no impact on the rate of [^{18}F]FDG phosphorylation, apoA-I pre-treatment further increased the rate of phosphorylation in insulin-treated animals ($3.55 \pm 1.05 \times 10^{-2} \text{ min}^{-1}$, $p < 0.05$). The influx constant (K_i) was not significantly different between PBS and apoA-I-treated mice (Fig. 4e). Similar to k_3 , pretreatment with apoA-I significantly increased the K_i in the insulin-treated animals compared with the PBS-treated animals ($3.70 \pm 0.65 \times 10^{-3}$ vs $2.01 \pm 0.28 \times 10^{-3} \text{ ml min}^{-1} \text{ g}^{-1}$, respectively; $p < 0.05$).

ApoA-I treatment increases hexokinase activity in vitro In an effort to understand the mechanism responsible for the

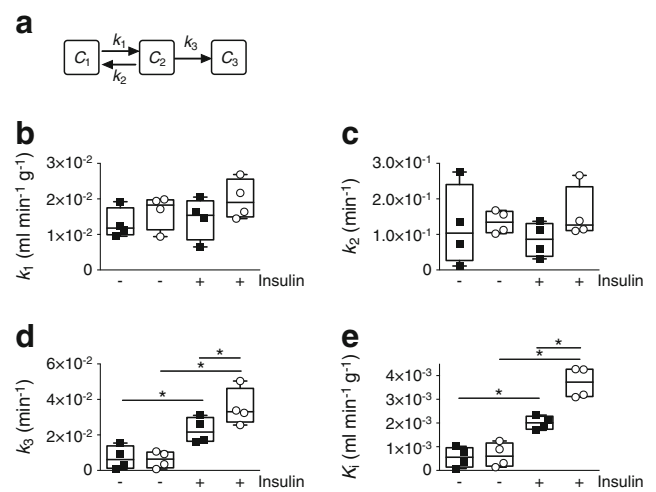


Fig. 4 Kinetic analysis of increased [^{18}F]FDG from plasma to gastrocnemius muscle in apoA-I-treated *db/db* mice. Time-activity curves were fitted to a two-tissue, three-compartment model (a) and used to determine the rate of transport of the tracer from the plasma compartment (C_1) to the intracellular space (C_2) (k_1) (b), rate of transport from intracellular space to plasma (k_2) (c), rate of [^{18}F]FDG phosphorylation (C_3) (k_3) (d) and the influx constant (K_i) (e). White circles, apoA-I-treated mice; black squares, PBS-treated controls. * $p < 0.05$

increased rate of [^{18}F]FDG phosphorylation in apoA-I-treated *db/db* mice, we examined the impact of apoA-I treatment on L6 rat skeletal muscle cells. Treatment of cells with apoA-I alone did not significantly increase hexokinase activity (Fig. 5a). Treatment with insulin significantly increased hexokinase activity ($100.00 \pm 8.32\%$ vs $192.01 \pm 8.32\%$ for PBS alone and PBS insulin-treated groups; $p < 0.001$) and was further increased in apoA-I-pretreated cells ($260.14 \pm 6.98\%$;

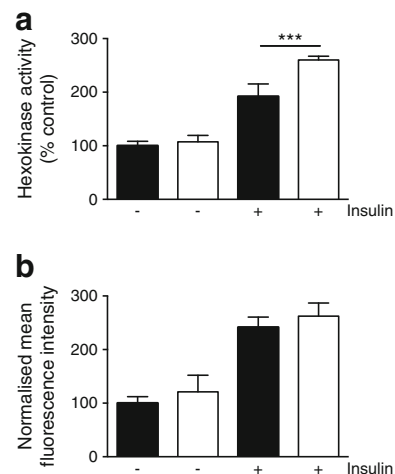


Fig. 5 ApoA-I treatment increases insulin-dependent hexokinase activity but not GLUT4 translocation in L6 rat skeletal muscle cells. (a) Hexokinase activity and (b) cell surface GLUT4 levels were determined in L6 rat skeletal muscle cells treated with apoA-I (1 mg/kg; white bars) or an equivalent volume PBS (black bars) for 1.5 h and then insulin (0.1 $\mu\text{mol/l}$) for a further 30 min. Values represent mean \pm SD ($n=3$) of two separate experiments. *** $p < 0.001$

$p < 0.005$ relative to PBS insulin alone). Treatment of L6 cells with insulin significantly increased cell surface GLUT4 levels ($100.00 \pm 12.22\%$ vs 241.54 ± 18.96) (Fig. 5b). However, treatment with apoA-I for 2 h had no impact on GLUT4 translocation, either in the presence or absence of insulin.

Discussion

In this study we have demonstrated that a single infusion of apoA-I significantly increases the rate of glucose uptake by skeletal muscle in *db/db* mice. Further, we have used real-time PET imaging to characterise the impact of apoA-I and insulin treatment on glucose uptake from the plasma into the gastrocnemius muscle in *db/db* mice. This proof of principle study has considerable flexibility and can be extended into studies of multiple organs and used longitudinally.

No significant increase in glucose uptake was observed when muscle samples were treated with insulin alone, which is a reflection of the insulin resistant state of *db/db* mice. Treatment of the mice with apoA-I alone significantly increased glucose uptake. When the mice were treated with apoA-I and the skeletal muscle was subsequently treated with insulin, glucose uptake was increased over and above that of apoA-I alone. This is indicative of apoA-I not only increasing the glucose uptake, but also improving insulin sensitivity. This is consistent with previous reports of apoA-I increasing skeletal muscle glucose uptake in both the presence and absence of insulin [2, 4].

HDL and apoA-I can activate a number of cell signalling pathways that have been linked to increased glucose uptake and insulin sensitivity. These include the AMP kinase pathway [21–27], which is known to be activated by apoA-I [4]. HDL can also activate phosphatidylinositol-3 kinase (PI3K)/Akt via scavenger receptor class B type I (SR-BI) [28], which increases the trafficking of GLUT4 from intracellular stores to the cell surface [6], thereby increasing cellular glucose uptake. We have also previously demonstrated that apoA-I can activate protein kinase A (PKA) [8], and PKA-mediated phosphorylation of peroxisome proliferator-activated receptor α has been shown to improve insulin sensitivity in rats [29]. The findings from the *ex vivo* skeletal muscle glucose uptake experiment suggested that apoA-I increased glucose uptake into skeletal muscle in an insulin-dependent and insulin-independent manner. To gain further insight into the impact of apoA-I treatment on glucose uptake and metabolism in skeletal muscle, we used kinetic analysis to model the uptake of [^{18}F]FDG from the plasma into the muscle. Rather than collecting numerous arterial blood samples during the PET study, which is impractical due to the small blood volume of mice, we derived the model input function from the reconstructed image data using an ROI over the vena cava [30]. To ensure the robustness of our variable estimates, PET

images were deconvolved to limit partial volume effects [16] and the dispersion of the input function was included as a fit variable during kinetic modelling. Mouse input functions have previously been determined using the whole heart [31] as well as heart, liver and a blood samples [32].

A limitation of our [^{18}F]FDG PET study is that it cannot determine whether small changes in k_1 are due to changes in blood flow in gastrocnemius tissue or altered glucose transport across the cell membrane. Multi-tracer approaches using [^{15}O]H $_2$ O and 3-*O*-[^{11}C]methylglucose together with [^{18}F]FDG have previously been used by other investigators to assess glucose delivery, transport and phosphorylation in humans [33–35]. However, due to the 2-min half-life of ^{15}O , this approach requires an on-site cyclotron and/or [^{15}O]H $_2$ O generator to enable immediate injection which was not feasible for the current study. Without the ability to independently measure blood flow using [^{15}O]H $_2$ O, a 3-*O*-[^{11}C]methylglucose PET scan would not add any additional useful information since, like [^{18}F]FDG, it cannot distinguish between flow dependent changes in delivery of tracer to the tissue and increased glucose transport across the cell membrane.

The time–activity curves for the gastrocnemius muscle of *db/db* mice treated with apoA-I showed increased uptake relative to control treatment in both the absence and presence of insulin. Furthermore, apoA-I and insulin treatment led to an increased rate of exit of [^{18}F]FDG from the plasma compartment into tissue, relative to mice treated with insulin alone. As the rate of [^{18}F]FDG uptake into the gastrocnemius (k_1) cannot account for this alone, it is likely to be due to increased cumulative whole body uptake, potentially via an HDL-mediated increase in production of the vasodilator endothelial nitric oxide synthase [36].

The rate of transport of [^{18}F]FDG into the intracellular space (k_1) did not increase significantly in mice treated with apoA-I, either in the absence or presence of insulin. However, a trend towards increased k_1 values in apoA-I-treated animals was observed and could warrant further investigation in a PET-water study using [^{15}O]H $_2$ O to specifically measure any transport effect mediated by apoA-I. However, as noted above, this requires an on-site [^{15}O]H $_2$ O generation capability in the imaging facility. While the sample size used in this study is small ($n=4$), it was sufficiently powered to clearly identify the effect of apoA-I treatment on both K_i and k_3 values.

While previous studies have suggested HDL can improve glucose transport via increasing cell surface GLUT4 levels [5, 6], these studies were conducted *in vitro* and did not observe increased glucose transport with apoA-I treatment. HDL has previously been reported to increase GLUT4 translocation to the cell surface via SR-BI and Akt [6]. However, apoA-I does not activate the Akt pathway [8] and this may explain the lack of a significant increase in k_1 *in vivo* and in L6 rat skeletal muscle cells treated with apoA-I.

While apoA-I treatment alone had no impact on the rate of [^{18}F]FDG phosphorylation (k_3), treatment with apoA-I significantly increased the rate of insulin-dependent glucose phosphorylation. This appears to be somewhat contradictory to previous findings that glucose transport is rate limiting for glucose disposal in skeletal muscle [34]. Hexokinase II (HK-II), the primary enzyme responsible for glucose phosphorylation in skeletal muscle, is phosphorylated by insulin-dependent activation of the Akt/PI3K signalling pathway, resulting in increased HK-II-mitochondrial association [37], which in turn increases HK-II activity [38–40]. Using the L6 rat skeletal muscle cell line, we confirmed that treatment of cells with apoA-I increased insulin-mediated HK-II activity, providing further evidence that while not able to activate the Akt/PI3K pathway directly, apoA-I potentiates insulin-mediated activation of HK-II activity. As such, this study suggests that the primary mechanism responsible for increased apoA-I-mediated insulin sensitivity is increased phosphorylation of glucose via increased potentiation of the insulin signalling pathway.

Funding This work was supported by a National Imaging Facility Subsidised Access Grant to BJC.

Duality of interest The authors declare that there is no duality of interest associated with this manuscript.

Contribution statement BJC was responsible for the experimental design, carried out the experiments, performed data analysis and wrote the manuscript. WJR was responsible for the experimental design, performed data analysis, and wrote the manuscript. AP, ST, AR, AA, AC and HH carried out the experiments, performed data analysis and revised the manuscript. PJB, LK, SRM, MCG and KAR were responsible for the experimental design and wrote the manuscript. All authors approved the final version of the manuscript for publication. BJC is the guarantor of this work and, as such, has full access to all the data in the study and takes responsibility for the integrity of the data and the accuracy of the data analysis.

References

- Drew BG, Rye KA, Duffy SJ, Barter P, Kingwell BA (2012) The emerging role of HDL in glucose metabolism. *Nat Rev Endocrinol* 8:237–245
- Drew BG, Duffy SJ, Formosa MF et al (2009) High-density lipoprotein modulates glucose metabolism in patients with type 2 diabetes mellitus. *Circulation* 119:2103–2111
- Barter PJ, Rye KA, Tardif JC et al (2011) Effect of torcetrapib on glucose, insulin, and hemoglobin A1c in subjects in the Investigation of Lipid Level Management to Understand its Impact in Atherosclerotic Events (ILLUMINATE) trial. *Circulation* 124:555–562
- Han R, Lai R, Ding Q et al (2007) Apolipoprotein A-I stimulates AMP-activated protein kinase and improves glucose metabolism. *Diabetologia* 50:1960–1968
- Dalla-Riva J, Stenkula KG, Petrova J, Lagerstedt JO (2013) Discoidal HDL and apoA-I-derived peptides improve glucose uptake in skeletal muscle. *J Lipid Res* 54:1275–1282
- Zhang Q, Zhang Y, Feng H et al (2011) High density lipoprotein (HDL) promotes glucose uptake in adipocytes and glycogen synthesis in muscle cells. *PLoS One* 6, e23556
- Fryirs MA, Barter PJ, Appavoo M et al (2010) Effects of high-density lipoproteins on pancreatic beta-cell insulin secretion. *Arterioscler Thromb Vasc Biol* 30:1642–1648
- Cochran BJ, Bisoendial RJ, Hou L et al (2014) Apolipoprotein A-I increases insulin secretion and production from pancreatic beta-cells via a G-protein-cAMP-PKA-FoxO1-dependent mechanism. *Arterioscler Thromb Vasc Biol* 34:2261–2267
- McGrath KC, Li XH, Whitworth PT et al (2014) High density lipoproteins improve insulin sensitivity in high-fat diet-fed mice by suppressing hepatic inflammation. *J Lipid Res* 55:421–430
- Stenkula KG, Lindahl M, Petrova J et al (2014) Single injections of apoA-I acutely improve in vivo glucose tolerance in insulin-resistant mice. *Diabetologia* 57:797–800
- Ruan X, Li Z, Zhang Y et al (2011) Apolipoprotein A-I possesses an anti-obesity effect associated with increase of energy expenditure and up-regulation of UCP1 in brown fat. *J Cell Mol Med* 15:763–772
- Kobayashi K, Forte TM, Taniguchi S, Ishida BY, Oka K, Chan L (2000) The db/db mouse, a model for diabetic dyslipidemia: molecular characterization and effects of Western diet feeding. *Metabolism* 49:22–31
- Yue P, Arai T, Terashima M et al (2007) Magnetic resonance imaging of progressive cardiomyopathic changes in the db/db mouse. *Am J Physiol Heart Circ Physiol* 292:H2106–H2118
- Hagberg CE, Mehlem A, Falkevall A et al (2012) Targeting VEGF-B as a novel treatment for insulin resistance and type 2 diabetes. *Nature* 490:426–430
- Sakamoto K, McCarthy A, Smith D et al (2005) Deficiency of LKB1 in skeletal muscle prevents AMPK activation and glucose uptake during contraction. *EMBO J* 24:1810–1820
- Tohka J, Reilhac A (2008) Deconvolution-based partial volume correction in Raclopride-PET and Monte Carlo comparison to MR-based method. *NeuroImage* 39:1570–1584
- Wu HM, Sui G, Lee CC et al (2007) In vivo quantitation of glucose metabolism in mice using small-animal PET and a microfluidic device. *J Nucl Med* 48:837–845
- Iida H, Kanno I, Miura S, Murakami M, Takahashi K, Uemura K (1986) Error analysis of a quantitative cerebral blood flow measurement using H $_2$ (15)O autoradiography and positron emission tomography, with respect to the dispersion of the input function. *J Cereb Blood Flow Metab* 6:536–545
- Oikonen V (2002) Model equations for the dispersion of the input function in bolus infusion PET studies. Available from www.turkupetcentre.net/reports/tpcm0003.pdf. Accessed 20 Mar 2015
- Koshy S, Alizadeh P, Timchenko LT, Beeton C (2010) Quantitative measurement of GLUT4 translocation to the plasma membrane by flow cytometry. *J Vis Exp*. doi:10.3791/2429
- Barnes BR, Ryder JW, Steiler TL, Fryer LG, Carling D, Zierath JR (2002) Isoform-specific regulation of 5' AMP-activated protein kinase in skeletal muscle from obese Zucker (fa/fa) rats in response to contraction. *Diabetes* 51:2703–2708
- Koistinen HA, Galuska D, Chibalin AV et al (2003) 5-Aminoimidazole carboxamide riboside increases glucose transport and cell-surface GLUT4 content in skeletal muscle from subjects with type 2 diabetes. *Diabetes* 52:1066–1072
- Song XM, Fiedler M, Galuska D et al (2002) 5-Aminoimidazole-4-carboxamide ribonucleoside treatment improves glucose homeostasis in insulin-resistant diabetic (ob/ob) mice. *Diabetologia* 45:56–65
- Bergeron R, Previs SF, Cline GW et al (2001) Effect of 5-aminoimidazole-4-carboxamide-1-beta-D-ribofuranoside infusion

- on in vivo glucose and lipid metabolism in lean and obese Zucker rats. *Diabetes* 50:1076–1082
25. Salminen A, Hyttinen JM, Kaamiranta K (2011) AMP-activated protein kinase inhibits NF-kappaB signaling and inflammation: impact on healthspan and lifespan. *J Mol Med* 89:667–676
 26. Steinberg GR, Kemp BE (2009) AMPK in health and disease. *Physiol Rev* 89:1025–1078
 27. Ruderman NB, Xu XJ, Nelson L et al (2010) AMPK and SIRT1: a long-standing partnership? *Am J Physiol Endocrinol Metab* 298: E751–E760
 28. Mineo C, Yuhanna IS, Quon MJ, Shaul PW (2003) High density lipoprotein-induced endothelial nitric-oxide synthase activation is mediated by Akt and MAP kinases. *J Biol Chem* 278:9142–9149
 29. Kou XH, Zhu MF, Chen D et al (2012) Bilobetin ameliorates insulin resistance by PKA-mediated phosphorylation of PPARalpha in rats fed a high-fat diet. *Br J Pharmacol* 165:2692–2706
 30. Thorn SL, deKemp RA, Dumouchel T et al (2013) Repeatable noninvasive measurement of mouse myocardial glucose uptake with [¹⁸F]FDG: evaluation of tracer kinetics in a type 1 diabetes model. *J Nucl Med* 54:1637–1644
 31. Alf MF, Wyss MT, Buck A, Weber B, Schibli R, Kramer SD (2013) Quantification of brain glucose metabolism by [¹⁸F]FDG PET with real-time arterial and image-derived input function in mice. *J Nucl Med* 54:132–138
 32. Tantawy MN, Peterson TE (2010) Simplified [¹⁸F]FDG image-derived input function using the left ventricle, liver, and one venous blood sample. *Mol Imaging* 9:76–86
 33. Bertoldo A, Pencek RR, Azuma K et al (2006) Interactions between delivery, transport, and phosphorylation of glucose in governing uptake into human skeletal muscle. *Diabetes* 55:3028–3037
 34. Goodpaster BH, Bertoldo A, Ng JM et al (2014) Interactions among glucose delivery, transport, and phosphorylation that underlie skeletal muscle insulin resistance in obesity and type 2 diabetes: studies with dynamic PET imaging. *Diabetes* 63:1058–1068
 35. Ng JM, Bertoldo A, Minhas DS et al (2014) Dynamic PET imaging reveals heterogeneity of skeletal muscle insulin resistance. *J Clin Endocrinol Metab* 99:E102–E106
 36. Yuhanna IS, Zhu Y, Cox BE et al (2001) High-density lipoprotein binding to scavenger receptor-BI activates endothelial nitric oxide synthase. *Nat Med* 7:853–857
 37. Roberts DJ, Tan-Sah VP, Smith JM, Miyamoto S (2013) Akt phosphorylates HK-II at Thr-473 and increases mitochondrial HK-II association to protect cardiomyocytes. *J Biol Chem* 288:23798–23806
 38. Vogt C, Yki-Jarvinen H, Iozzo P et al (1998) Effects of insulin on subcellular localization of hexokinase II in human skeletal muscle in vivo. *J Clin Endocrinol Metab* 83:230–234
 39. Kruszynska YT, Mulford MI, Baloga J, Yu JG, Olefsky JM (1998) Regulation of skeletal muscle hexokinase II by insulin in nondiabetic and NIDDM subjects. *Diabetes* 47:1107–1113
 40. Calmettes G, John SA, Weiss JN, Ribalet B (2013) Hexokinase-mitochondrial interactions regulate glucose metabolism differentially in adult and neonatal cardiac myocytes. *J Gen Physiol* 142: 425–436